

Various High Density Point Cloud Registration Results Analysis in Heritage Building (Penataran Temple, Penglipuran Village, Bali)

Asep Yusup Saptari^{a,*}, Ratri Widyastuti^a, Hamdani^a

^a *Geodesy and Geomatics Engineering, Bandung Institute of Technology, Jl. Ganesa 10, Bandung, 40132, Indonesia*

*Corresponding author: *aysaptari@gmail.com*

Abstract— 3D modeling of functional buildings is growing rapidly because of its excellence. 3D modeling can also be applied to heritage buildings, but it is still rarely done due to the variety of detail, and the unique shape of the objects in heritage buildings make it more difficult to be modeled. In consequence, an adequate instrument with different scanning densities is required in this case, namely Terrestrial Laser Scanner (TLS) and Handheld Laser Scanner (HLS). This study, conducted at Penataran Temple in Penglipuran Village, Bali, aims to analyze the registration result of point clouds acquired by TLS and HLS, as well as its capability to build the 3D model. Point cloud data is acquired using TLS and HLS tools, and the information about the object is obtained by doing interviews with the Chief of Penglipuran Village and the villagers. The point cloud that TLS acquires is registered with Iterative Closed Point (ICP) algorithm, while the point cloud of HLS is registered by using Helmert and Affine transformation method. Based on the results, the registration of HLS point cloud data to the TLS Affine method has better quality accuracy than the Helmert method. In addition, point cloud data scanned by HLS can present 3D models with a better Level of Detail (LOD) than point cloud data from TLS.

Keywords—Heritage building; Terrestrial Laser Scanner (TLS); Handheld Laser Scanner (HLS); point cloud.

Manuscript received 1 Jul. 2021; revised 16 Sep. 2021; accepted 15 Feb. 2022. Date of publication 31 Oct. 2022. IJASEIT is licensed under a Creative Commons Attribution-Share Alike 4.0 International License.



I. INTRODUCTION

At the end of the last century, quick development in information technology has taken place, and architectural representation procedures have been affected by it under the name of Building Information Modeling (BIM) [1]–[3]. BIM is typically best suited and mostly applied for new construction[4] rather than to existing ones. It may happen because the effort of modeling and converting to smart objects is high [1] and as the parametric objects of the available software are unable to adapt to the morphological irregularities that are common in historical structures [4], [5]. But since it is one of the most reliable methods for building documentation, it ultimately broadens the possibility of using BIM in historical and heritage environments [6]. Over the past years, the significance of digital recording of cultural heritage has been realized as a major factor in the preservation and dissemination of culture [7]. Segmentation of information, incomplete details, and poor record keeping are some of the factors that affect the pursuit of preserving one cultural values in a building [8].

A new approach to the cataloging of architectural heritage is proposed, thanks to the use of technologies that allow storing

information in the same model as the HBIM (Historic Building Information Modeling) [9]. By combining quantitative (geometric) and qualitative (non-geometric) data, BIM modeling can be carried out to see changes in the past and see the future and can be used to manage cultural heritage buildings and landscapes [10]. BIM allows planning, management, maintenance, and restoration of buildings to be carried out in an integrated manner.

Many surveying techniques are available for acquiring data needed to generate an accurate as-built 3D model [11], including laser scanning; Laser scanning is a system that can operate methodically at the speed of acquisition and possibly access data in real time[11]. This study uses Terrestrial Laser Scanner (TLS) and Handheld Laser Scanner (HLS). In recent years, the use of TLS seems to be increasing as its effectiveness in recording and documenting cultural heritage is widely documented [12]. Generally, TLS suffers from partial occlusion [13]; TLS can not capture some parts of the object due to the limited field of view of the scanner [14] since it is a static laser. However, there is HLS, an optimal supplement to TLS [15], which can scan large-scale objects/models by recording hidden areas in conjunction with TLS on the one hand or scanning small artifacts on the other

[16]. A handheld 3D scanning device introduces unique flexibility at high accuracy levels, and it can, thus, be considered a highly applicable device in the delicate area of heritage archiving [7].

Both of these technologies can scan objects with accuracy up to mm with the output in the form of a collection of data points that make up the object called a point cloud. However, the difference in density between the two tools raises questions about the quality of the point cloud results and the model formed. This study was conducted to analyze the results of the TLS and HLS point cloud data registrations and the 3D models that can be presented from the two data. There are several modeling standards in BIM, one of which is the Level of Development (LOD). Conceptually, LOD can be determined based on the level of detail of the element geometry (Level of Detail) combined with the level of information to be presented (Level of Information). By representing the model with multiple levels of detail (LoD), it is possible to provide appropriate visualization and efficient data access [17] [18]. With the data acquisition results that have different variations in detail, a 3D model of each object element can then be formed, and the LOD value can be determined.

The object of this study is Penataran Temple in Penglipuran Village in Bali. Bali is one of the provinces in Indonesia that holds many traditions and cultural heritage as a tourist attraction. One of them is heritage buildings such as Penataran Temple. The unique shape of the building with various kinds of heirloom objects has its charm for tourists. Each part of the building has its function and meaning. Seeing the great tourism potential of this cultural heritage and concerns about damage to heritage buildings, a digital inventory using HBIM is needed.

II. MATERIALS AND METHOD

Point cloud data retrieval is acquired using laser scanner technology, namely Terrestrial Laser Scanner Topcon GLS-2000 and Handheld Laser Scanner Stonex F6. There are four stages carried out in this research are as follows:

A. Data Acquisition

The data acquisition conducted includes taking point cloud data to form 3D models and semantic data of heritage buildings. Before doing the scanning process with TLS and HLS, two control points were measured using the Global National Satellite System (GNSS) method with two receivers. This receiver has an accuracy of $2.5 \text{ mm} \pm 1 \text{ ppm RMS}$ for horizontal and $5 \text{ mm} \pm \text{ppm RMS}$ for vertical. Measurements were conducted in 180 minutes about CORS Dasan Agung.

Then, Penataran Temple was scanned using TLS with a density of 12.5mm. HLS is used to scan one of the statue's details on the front of Penataran Temple at a distance of 0.5-1 m from the object. Point cloud data acquisition on TLS uses the concept of laser scanning with scanning methods like traverse scans and free scans. TLS uses laser technology such as LiDAR (Light Detection And Ranging) to measure objects and their surroundings to produce a point cloud [19] which is a collection of XYZ coordinates in a general coordinate system that describes the spatial distribution of an object [20]. The Stonex F6 SR works with an emitter projecting a near infrared (NIR) light through Mantis Vision's proprietary pattern onto the scene while a receiver calculates the distance of each

mapped point through triangulation algorithm and of the 3D scene by stereoscopic parallax [21]. HLS provides high mobility, limited operational cost, and reduced data collection time [19] and can be applied to many needs, including cultural heritage [22]. Meanwhile, for semantic data, data collection was obtained by doing interviews with the Chief of Penglipuran Village and the villagers.

B. Point Cloud Data Processing

Point cloud data processing is carried out in several stages: 1) georeference, 2) noise filtering, and 3) registration. The first stage is to georeference the point cloud to a global coordinate system using Magnet Collage software. In this study, the georeferencing process produces point cloud data with a 50S Zone UTM projection coordinate system. The binding stage on the UTM system is carried out so that 3D objects can be combined with other data already existing in the same system. The second stage is noise filtering, which eliminates unnecessary point clouds. The software used in this noise filtering process is Maptek i-site studio.

The last stage is point cloud registration. Most objects will require multiple scans from multiple angles to capture the entire surface, and each scan must be registered in order to be able to create a 3D model [23]. The multi-viewpoint clouds in different coordinate systems should be transformed into one coordinate system. This process is called point cloud registration [5], [22]-[23], [25], [27]-[30]. TLS scanned point cloud data is registered using the cloud-to-cloud registration method, which requires a 30% patch area. This method uses manual translation, and rotation processes are carried out by selecting an allied point between the two data point clouds. The Iterative Cloud Point (ICP) algorithm continues the registration process. The ICP algorithm builds a transformation matrix by finding the point-to-point correspondence between two-point cloud datasets and aligning the two-point cloud datasets accurately through iterations [3], [24], [25].

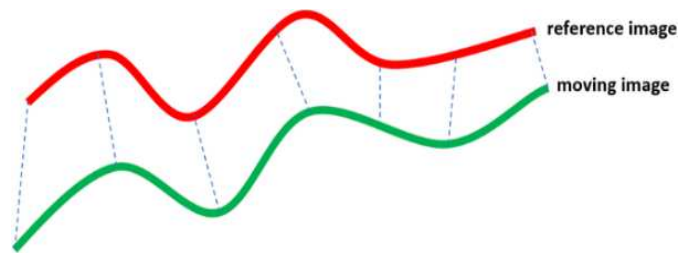


Fig. 1 ICP algorithm illustration [31]

In Fig. 1, the red line is the reference point cloud, while the green line is the target cloud point to be registered. This process produces a registered point cloud data along with the Root Mean Square Error (RMSE) as a representation of the quality of the registration [32]; the RMSE can be calculated using the following equation:

$$RMS_e = \sqrt{(RMS_x)^2 + (RMS_y)^2 + (RMS_z)^2} \quad (1)$$

RMS_x , RMS_y , RMS_z , and RMS_e are the error values on the registration results' x,y,z axes, and the total. There is a specified tolerance value in conducting measurements and calculations of RMSE. The value of the error tolerance based

on the 95% confidence level can be determined using the following equation [33]:

$$\text{Error Tolerance Value} = 1.960\sigma \quad (2)$$

σ is single point positional accuracy (SPA). The SPA value can be calculated using the following equation [33]:

$$\sigma = \sqrt{dx^2 + dy^2 + dz^2} \quad (3)$$

The values of dx, dy, and dz are the errors on the x, y, and z axes. In addition to using equation (3), the SPA value can also be seen from the tools' specifications.

Because the point cloud data from the HLS scan is registered with the point cloud from TLS, which has different densities, the Helmert and Affine 3-dimensional transformation methods are used to combine the two data. The Helmert and Affine transformation method selection in this study is based on the Helmert transformation [34] and the Affine transformation [35]. The parameters used are small, so the minimum number of common points required is also small, the equation model is simple, the Helmert transform has conform properties, while the Affine transformation has non conform properties. These two methods can also be used to see whether the HLS scanned point cloud has a shape that matches the original object.

C. Creating 3D Models and BIM

3D modeling and BIM creation were carried out using Autodesk Revit 2018 software. The 3D model of Penataran Temple was formed with Level of Development (LOD) object elements that vary depending on the LoD and information to be presented. In the BIM community, Levels Of Detail (LoD) and Level Of Development (LOD) is now crucial concepts that have to be integrated globally way to standardize the description of information [36]–[38]. The steps taken are making a family and making a project. Objects are created with self-defined parameters and references in the family creation stage.

The 3D model of the HLS point cloud data is formed using automatic vectorization, namely the Mesh Model. This model is formed from a collection of every three adjacent points that are connected into a triangle, which produces a continuous triangular net on the surface of the object [39], as can be seen in Fig. 6. After the family is formed, the next step is making a project, namely making a complete 3D model of an area. The making of the project is performed using the model from the family as a reference to form a complete building system according to the research area. Since the project creation is complete, information about the building can be entered into each element/object in the project. Provision of information is done using the "shared parameter" tool. Information entered into a 3D model must have attributes that refer to Industry Foundation Classes (IFC). In this study, the IFC Object was used as a reference.

D. Validation

The method used in this study is visual validation, which compares the shapes and colors of the 3D model with the original object.

III. RESULT AND DISCUSSION

A. TLS Data Point Cloud Registration

The RMSE value in the TLS scanned point cloud dataset registration calculated by the Iterative closest point (ICP) algorithm is 0.0316 mm for each pair of scanning results. The TLS tool used by the GLS-2000 type has a single point positional accuracy (SPA) of 3.5 mm at a distance of 1 to 90 m. Using equation (2), the RMSE tolerance obtained is 1.960 times 3.5 mm, which is 6.86 mm, so the RMSE value meets the specified tolerance limit.

Based on equation (1), it can be seen that the RMSE value depends on the suitability of the x, y, and z coordinate values, between paired point clouds and the amount of data used. The suitability of the x, y, and z coordinate values can be influenced by the percentage of overlap between the two datasets of point cloud, while the sample size represents the amount of data used in the calculation. The higher the percentage of overlap between the two datasets of point cloud, the better the RMSE value obtained. The number of samples used in each calculation of each dataset is 1000 points and the average percentage of overlap between point cloud datasets in this study is 79.69%.



Fig. 2 Visualization of TLS Data Registration Results

B. HLS Point Cloud Data Registration Against TLS Point Cloud Data

After the TLS point cloud data has been registered and has the appropriate coordinates, the HLS point cloud data registration process is carried out for the registered TLS point cloud. This is done because the HLS tool does not have a positioning device, such as GPS, so the coordinates of the resulting cloud points are still in the local coordinate system. Unlike the registration of TLS data, HLS data is registered with the Helmert and Affine transformation methods. These two methods are commonly used in coordinate transformation, and both were chosen to compare the recording results obtained. The ICP method was not chosen because the TLS point cloud data density with HLS is different, thus allowing errors in determining cloud point pairs if using the ICP algorithm.

The registration process begins with determining the allied points between the two point cloud datasets (TLS and HLS). The common point is the point that is considered the same between the two data point clouds. In this study, the number of allied points determined was 6 points. This number was chosen because it can meet the minimum needs of allies in using the Affine transformation method. The common point is determined naturally, that is, using the observer's perception. The following is a visualization of the selected allied points:

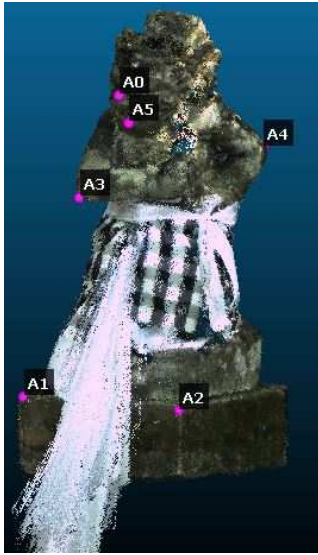


Fig. 3 Allies point distribution

The RMSE value of the Helmert method transformation carried out on the HLS scanned point cloud dataset is 0.168 m, while the RMSE of the Affine method is 0.005 m.

TABLE I
HELMERT AND AFFINE COORDINATE TRANSFORMATION RESULTS

Point	Helmert			Affine		
	V _x (m)	V _y (m)	V _z (m)	V _x (m)	V _y (m)	V _z (m)
1	-0.025	0.132	-0.057	-0.004	0.001	-
2	0.072	-0.165	0.075	0.004	-0.003	0.003
3	-0.065	0.209	0.023	-0.004	0.002	-
4	0.02	-0.02	-0.009	-0.002	-0.004	0.003
5	0.011	-0.233	0.007	0.005	0.002	0.003
6	-0.012	0.077	-0.039	0.001	0.002	0.001

As shown in Table 1, the residual value or deviation of the Helmert method transformation varies from mm to cm. The large residual value is on the y-axis, which ranges from 2 cm to 23 cm. In Table 1, the residual values obtained also vary but tend to be small and similar, ranging from 1 to 5 mm. By using equation (1), the RMSE value of each transformation method can be calculated. The following are the RMSE results obtained:

TABLE II
RMSE TRANSFORMATION RESULT OF HELMERT'S METHOD

RMS _x (m)	RMS _y (m)	RMS _z (m)	RMSe (m)
0.042228	0.157558	0.042922	0.168671

TABLE III
RMSE TRANSFORMATION RESULT OF AFFINE'S METHOD

RMS _x (m)	RMS _y (m)	RMS _z (m)	RMSe (m)
0.003606	0.002517	0.002517	0.005066

As can be seen in Table 2 and 3, the RMSE produced by the coordinate transformation of the Affine method is smaller than that of the Helmert method. The RMSE of the Helmert method

is 0.168 m or about 16.8 cm, while the RMSE of the Affine method is 0.005 m or 5 mm.

Table 4 below shows that HLS point cloud registration results from the Helmert and Affine coordinate transformation methods are not much different. However, when overlaid with TLS point cloud data, it appears that the size or dimensions of the Helmert method transformation results of HLS point cloud data do not match the TLS point cloud data. In the visualization of the results of the Affine transformation method, it can be seen that the HLS and TLS point clouds overlap neatly, and the dimensions are also appropriate.

TABLE IV
HELMERT AND AFFINE TRANSFORMATION RESULTS VISUALIZATION

Method	Shape	Overlay with TLS
Helmert		

C. Visualization of 3D Models and Attributes

The size of the 3D model that is formed already refers to the TLS scanned point cloud data. Then the results are integrated into the project into a unified whole object.



Fig. 4 3D model of TLS point cloud on Autodesk Revit

Unlike the TLS point cloud, HLS scanned data cannot be modeled manually because the density is higher and the object being modeled has curves that are quite difficult to model

manually. Therefore, the modeling of mesh type with 1000 triangles used was carried out so that the results adequately represent the object's shape. The first step that can be done to create a mesh model is to calculate the "normal" of the point clouds. This "normal" calculation is done by determining the type of surface model that wanted to be used, the distance to identify the neighborhood, and the orientation.

The type of surface model used in this modeling is "plane," a surface model that is usually the most suitable for mesh modeling. This surface model can reduce noise to the maximum but is not good for objects that have sharp edges and corners. Then, the distance used to identify the neighborhood is 0.012382 m, which determines how many points are used in computing the surface model.

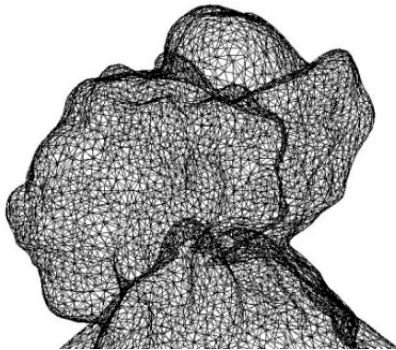


Fig. 5 Triangular planar visualization in model

The mesh model can then be formed using the "PoissonRecon" (Poisson Surface Reconstruction) feature, which is a simple interface used in the triangular net-making algorithm. This whole process is applied to the making of the statue's model and the sarong it uses (*saput poleng*).



Fig. 6 Mesh model result



Fig. 7 3D model visualization of HLS point cloud

In order to build a 3D database for all object elements, information is added to the object elements in the form of names, meanings, and functions obtained from interviews conducted. A connection with database software is needed to maximize the function of a 3-dimensional database so that attribute data containing information about objects can be integrated with 3D objects such as Microsoft Access.

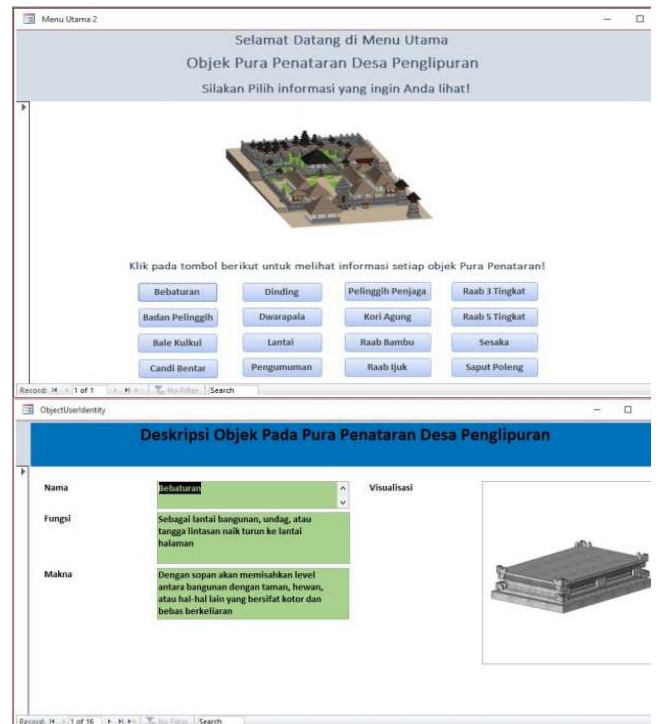


Fig. 8 Main menu form display and object description

The added attributes refer to the Industry Foundation Classes (IFC) standard, customized to the needs. The type of IFC used is IFC Object because the information displayed on the model is the basic information of the object. The information displayed on the object elements is the name, meaning, and function obtained from the interviews with the Chief of Penglipuran Village and literature studies. The results of these tables are then adjusted to the Entity Relationship (ER) diagram.

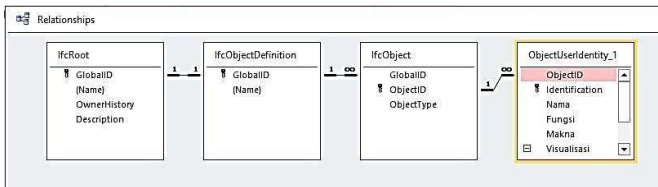


Fig. 9 Entity relationship diagram

IV. CONCLUSION

The results of HLS point cloud data registration for TLS using the Affine method have better quality accuracy with a small RMSE value, with units up to millimeters, compared to the Helmert method with RMSE up to centimeters. The point cloud scanned by HLS can present 3D models up to Level of Detail 4 and Level of Development 350, while the scanned TLS can present 3D models with Level of Detail 3 and Level of Development 350. In other words, 3D models that the resulting point clouds HLS scans can present have a higher level of detail than TLS, providing deeper information about objects.

D. Level of Detail, Level of Information, and Level of Development

Almost all object elements have a Level of Information (LOI) of 500 because the Penglipuran Village Customary Chief provides additional information. There is only one element with an LOI value of 300: the floor and grass.

TABLE V
LEVEL OF DEVELOPMENT RESULT OF THE OBJECT

Items	Level of Detail	Level of Information	Level of Development
Sesaka	3	500	300
Raab Bambu	3	500	300
Raab Ijuk	3	500	300
Raab 3 Tingkat pada Pelinggih Meru	3	500	300
Raab 5 Tingkat pada Pelinggih Meru	3	500	300
Bebaturan pada Bale Banjar	3	500	300
Bebaturan Tangga	3	500	300
Bebaturan pada Pelinggih di zona "Utama Ning Utama"	3	500	300
Candi Bentar	3	500	300
Candi Kori	3	500	300
Pelinggih Penjaga Pura	3	500	300
Bulletin board	3	500	300
Bale Kulkul	3	500	300
Dwarapala	4	500	350
Saput Poleng	4	500	350
Wall	3	500	300
Floor and grass	2	300	300

In reference to Table 5, the LoD value varies from 2 to 4, with a value of 2 only on one object. This is because the floor and grass are only modeled with simple shapes. The value of LoD 4 is due to the TLS scanned point cloud data that does not have sufficient density to form very deep object details and the limited ability of human resources to model objects manually due to the complexity of object element shapes. The value of LoD 4 on sculpture objects and *saput poleng* is generated by HLS scanned point cloud data which has a very high density.

E. Visual Comparison

There is a conformity of the shape of the 3D model with the original object based on shape and color.



Fig. 10 Visual validation

The RMSE value is numerically greater than the density of the point cloud from the HLS device, but this study proves that the point cloud generated by the HLS tool can be integrated with the point cloud from TLS so that it can produce a complete 3D object and more detailed information can also be added on objects with a denser level of detail. In this study, only one type of the number of allied points was used in the registration process, which is six points, and produced a fairly good RMSE value in the Affine method. In future research, it can be added and/or reduced the number of allied points in the Affine registration process intending to analyze the effect of the number of allied points on the quality of the registration results and how big the difference in the registration results is when compared to the ICP algorithm.

REFERENCES

- [1] D. P. Pocobelli, J. Boehm, P. Bryan, J. Still, and J. Grau-Bové, "BIM for heritage science: a review," *Herit. Sci.*, vol. 6, no. 1, pp. 23–26, 2018, doi: 10.1186/s40494-018-0191-4.
- [2] J. Sun, S. Mi, P. Olsson, J. Paulsson, and L. Harrie, "Utilizing BIM and GIS for Representation and Visualization of 3D Cadastre," 2019.
- [3] S. Hendriatiningsih, A. Hernandi, A. Y. Saptari, R. Widyastuti, and D. Saragih, "Building Information Modeling (BIM) Utilization for 3D Fiscal Cadastre," *Indones. J. Geogr.*, vol. 51, no. 3, pp. 285–294, 2019.
- [4] F. Banfi, L. Chow, M. R. Ortiz, and S. Fai, "Building Information Modeling for Cultural Heritage: The Management of Generative Process for Complex Historical Buildings Building Information Modeling for Cultural Heritage: The Management of Generative Process," in *Digital Cultural Heritage*, no. May, 2018, pp. 119–130.
- [5] Y. Alshwabkeh, A. Baik, and Y. Miky, "Integration of Laser Scanner and Photogrammetry for Heritage BIM Enhancement," *Int. J. Geo-Information*, vol. 10, no. 5, p. 316, 2021.
- [6] M. Murphy, E. MCGovern, and S. Pavia, "Historic building information modelling (HBIM)," *ISPRS J. Photogramm. Remote Sens.*, vol. 76, no. February 2013, pp. 89–102, 2009, doi: 10.1108/02630800910985108.
- [7] F. Arnaoutoglou, A. Koutsoudis, G. Pavlidis, V. Tsioukas, and C. Chamzas, *Towards a versatile handheld 3D Laser Scanner, The 7th International Symposium on Virtual Reality, Archaeology and Cultural Heritage (VAST 2006)*, Nicosia, Cyprus, 30 October - 4 November, 2006, pp 7-12. 2006.
- [8] M. Ali, K. Ismail, K. Has-Yun Hashim, S. Suhaimi, and H. Mustafa, "Heritage building preservation through building information modelling: Reviving cultural values through level of development exploration," *Plan. Malaysia J.*, vol. 16, Sep. 2018, doi: 10.21837/pmjournal.v16.i6.461.
- [9] L. Hernández and M. Quintilla Castán, *Virtual Reconstruction in BIM Technology and Digital Inventories of Heritage*. 2019.
- [10] S. Fai, K. Graham, T. Duckworth, N. Wood, and R. Attar, *Building Information Modeling and Heritage Documentation*. 2011.
- [11] G. Vacca, M. Deidda, A. Dessi, and M. Marras, "Laser Scanner Survey to Cultural Heritage Conservation and Restoration," *ISPRS - Int. Arch. Photogramm. Remote Sens. Spat. Inf. Sci.*, vol. XXXIX-B5, pp. 589–594, Jul. 2012, doi: 10.5194/isprsarchives-XXXIX-B5-589-2012.
- [12] O. C. Wei, C. S. Chin, Z. Majid, and H. Setan, "3D Documentation and Preservation of Historical Monument Using Terrestrial Laser," *Geoinf. Sci. J.*, vol. 10, no. 1, pp. 73–90, 2010.

- [13] E. Kempter, C. Cogima, P. Paiva, M. Antonio, and M. Carvalho, *BIM for Heritage Documentation An ontology-based approach*. 2018.
- [14] C. Balletti and M. Ballarin, "An Application of Integrated 3D Technologies for Replicas in Cultural Heritage," *ISPRS International Journal of Geo-Information*, vol. 8, no. 6. 2019, doi: 10.3390/ijgi8060285.
- [15] T. Kersten, H.-J. Przybilla, and M. Lindstaedt, "Investigations of the Geometrical Accuracy of Handheld 3D Scanning Systems," *Photogramm. - Fernerkundung - Geoinf.*, vol. 2016, pp. 271–283, Dec. 2016, doi: 10.1127/pfg/2016/0305.
- [16] T. Kersten, H.-J. Przybilla, M. Lindstaedt, F. Tschirschwitz, and M. Misgaiski-Hass, *Comparative Geometrical Investigations of Hand-Held Scanning Systems*, vol. XLI-B5. 2016.
- [17] R. Akmalia, H. Setan, Z. Majid, and D. Suwardhi, "Representing 3D model of building from TLS data scanning in CityGML," *J. Teknol.*, vol. 71, no. 4, pp. 49–53, 2014, doi: 10.11113/jt.v71.3825.
- [18] R. Scopigno, M. Callieri, M. Dellepiane, F. Ponchio, and M. Potenziani, "Delivering and using 3D models on the web: Are we ready?," vol. 8, pp. 1–9, Jul. 2017, doi: 10.4995/var.2017.6405.
- [19] C. Stal, J. Verbeurgt, L. De Sloover, and A. Wulf, "Assessment of handheld mobile terrestrial laser scanning for estimating tree parameters," *J. For. Res.*, vol. 32, Sep. 2020, doi: 10.1007/s11676-020-01214-7.
- [20] C. Boardman *et al.*, *3D Laser Scanning for Heritage. Advice and Guidance on the Use of Laser Scanning in Archaeology and Architecture*. 2018.
- [21] G. Patrucco, F. Rinaudo, and A. Spreafico, "A New Handheld Scanner for 3D Survey of Small Artifacts: The Stonex F6," *Int. Arch. Photogramm. Remote Sens. Spat. Inf. Sci. - ISPRS Arch.*, vol. 42, no. 2/W15, pp. 895–901, 2019, doi: 10.5194/isprs-archives-XLII-2-W15-895-2019.
- [22] A. B. Azeez and A. M. Shrawai, "Low Cost Handheld 3D Scanning for Egyptian Architectural Artifacts Acquisition," *Int. J. Innov. Technol. Explor. Eng.*, vol. 9, no. 8, pp. 195–200, 2020, doi: 10.35940/ijitee.H6268.069820.
- [23] M. Wachowiak and B. Karas, "3d Scanning and Replication for Museum and Cultural Heritage Applications," *J. Am. Inst. Conserv.*, vol. 48, pp. 141–158, Aug. 2009, doi: 10.1179/019713609804516992.
- [24] A. D. Murtiyoso, "Geospatial Recording and Point Cloud Classification of Heritage Buildings," University of Strasbourg, 2020.
- [25] P. Jauer, I. Kuhlemann, R. Bruder, A. Schweikard, and F. Ernst, "Efficient registration of high-resolution feature enhanced point clouds," *IEEE Trans. Pattern Anal. Mach. Intell.*, vol. 41, no. 5, pp. 1102–1115, 2019, doi: 10.1109/TPAMI.2018.2831670.
- [26] T. Urbančič, Ž. Roškar, M. K. Fras, and D. Grigillo, "New target for accurate terrestrial laser scanning and unmanned aerial vehicle point cloud registration," *Sensors*, vol. 19, no. 14, pp. 1–29, 2019, doi: 10.3390/s19143179.
- [27] J. Lu, Z. Wang, B. Hua, and K. Chen, "Automatic point cloud registration algorithm based on the feature histogram of local surface," *PLoS One*, vol. 15, no. 9, p. e0238802, Sep. 2020.
- [28] P. Li, R. Wang, Y. Wang, and W. Tao, "Evaluation of the ICP Algorithm in 3D Point Cloud Registration," *IEEE Access*, vol. 8, pp. 68030–68048, 2020, doi: 10.1109/ACCESS.2020.2986470.
- [29] F. Bosché, "Plane-based registration of construction laser scans with 3D / 4D building models," *Adv. Eng. Informatics*, vol. 26, pp. 90–102, 2012, doi: 10.1016/j.aei.2011.08.009.
- [30] L. Yan, J. Tan, H. Liu, H. Xie, and C. Chen, "Automatic registration of TLS-TLS and TLS-MLS point clouds using a genetic algorithm," *Sensors (Switzerland)*, vol. 17, no. 9, 2017, doi: 10.3390/s17091979.
- [31] A. Kurniawan *et al.*, "Determining the effective number and surfaces of teeth for forensic dental identification through the 3D point cloud data analysis," *Egypt. J. Forensic Sci.*, vol. 10, Dec. 2020, doi: 10.1186/s41935-020-0181-z.
- [32] S. Damodaran, A. P. Sudheer, and T. K. S. Kumar, "An evaluation of spatial mapping of indoor environment based on point cloud registration using Kinect sensor," in *2015 International Conference on Control, Communication and Computing India, ICCCI*, 2015, pp. 548–552, doi: 10.1109/ICCC.2015.7432958.
- [33] A. Nandaru, B. Sudarsono, and B. D. Yuwono, "Jurnal Geodesi Undip Oktober 2014 Terrestrial Laser Scanner (TLS)," *Jurnal*, vol. 3, no. 4, pp. 201–211, 2014.
- [34] C.-O. Andrei, "3D affine coordinate transformations," Mar. 2006.
- [35] J. Niederoest, "3D Reconstruction and Accuracy Analysis of Historical Relief Models," in *3rd International Seminar on Development in Digital Photogrammetry*, 2001, pp. 3–5.
- [36] R. Alshorafa and E. Ergen, "Determining the level of development for BIM implementation in large-scale projects," *Eng. Constr. Archit. Manag.*, vol. 28, no. 1, pp. 397–423, Jan. 2021, doi: 10.1108/ECAM-08-2018-0352.
- [37] A. Y. Saptari, S. Hendriatiningsih, A. Hernandi, Sudarman, P. Rahmadani, and Saragih, "Level of Detail Analysis for Property and Building Information Modelling (BIM) Integration," *Int. J. Geoinformatics*, vol. 16, no. 2, 2020.
- [38] C.-E. Tolmer, C. Castaing, Y. Diab, and D. Morand, "Adapting LOD definition to meet BIM uses requirements and data modeling for linear infrastructures projects: using system and requirement engineering," *Vis. Eng.*, vol. 5, Dec. 2017, doi: 10.1186/s40327-017-0059-9.
- [39] H. M. Sharif, H. Hazumi, and R. H. Meli, "3D documentation of the petalaindera: digital heritage preservation methods using 3D laser scanner and phot," 2018, doi: 10.1088/1757-899X/290/1/012071.